

FIRST STEP TOWARD MODEL-FREE, ANONYMOUS OBJECT TRACKING WITH RECURRENT NEURAL NETWORKS

Quan Gan^{*◇}Qipeng Guo^{*◇}Zheng Zhang^{**}Kyunghyun Cho^{*◇}

ABSTRACT

In this paper, we propose and study a novel visual object tracking approach based on convolutional networks and recurrent networks. The proposed approach is distinct from the existing approaches to visual object tracking, such as filtering-based ones and tracking-by-detection ones, in the sense that the tracking system is explicitly trained off-line to track *anonymous* objects in a noisy environment. The proposed visual tracking model is end-to-end trainable, minimizing any adversarial effect from mismatches in object representation and between the true underlying dynamics and learning dynamics. We empirically show that the proposed tracking approach works well in various scenarios by generating artificial video sequences with varying conditions; the number of objects, amount of noise and the match between the training shapes and test shapes.

1 INTRODUCTION

Visual object tracking is a problem of building a computational model that is able to predict the location of a designated object from a video clip consisting of many consecutive video frames. Using deep learning techniques, we attack this problem with a model-free statistical approach.

Our goal in this paper is to build a model that can track an *anonymous* object in an image sequence. This task finds immediate applications in important scenarios such as self-driving cars. As safety is first-order consideration, identifying what class the object belongs to is much less critical than identifying their whereabouts to avoid a collision. It is also an important step towards dramatically improving the generalizability of a tracking system, since real-world objects far exceeds labelled categories.

Our model integrates convolutional network with recurrent network, and deploys attention at multiple representation layers. The recurrent network outputs a bounding box prediction of the target object. It fuses past predictions along with their corresponding visual features produced by the convolutional network. Finally, the prediction can optionally emphasizes attention areas in the input before feeding it into convolutional network. The entire model is end-to-end trained off-line. We use synthesized data set that simulates changing trajectory and acceleration of the target, various degree of foreground occlusions, and distraction of background clutter and other targets. Experimental results show that our model delivers robust performance.

The rest of the paper is organized as follows. We start by reviewing two important categories of conventional visual object tracking in Sec. 2, which are filtering-based tracking and tracking-by-detection. In Sec. 3, we describe a novel recurrent tracking model we propose in this paper, followed by discussing related works in Sec. 3.4. The settings for experiments are extensively described in Sec. 4–5, which is followed by the results and analysis in Sec. 6. We finalize this article with potential future research directions in Sec. 7.

* Equal contribution

◇ Fudan University, Shanghai

qgan11@fudan.edu.cn, guoqipeng831@gmail.com

• Courant Institute of Mathematical Sciences, New York University {zz, kyunghyun.cho}@nyu.edu

* NYU Shanghai

○ Center for Data Science, New York University

2 BACKGROUND: VISUAL OBJECT TRACKING AND LIMITATIONS

A system for visual object tracking often comprises two main components; object detection and object tracking. Object detection refers to the process by which a designated object in each video frame is detected, while object tracking refers to the process of continually predicting the location of the detected object.

The goal of *object detection* is to extract a feature vector $\phi(x)$ of an object which often encodes both the object’s shape and location, given each video frame x . The specifics of the feature vector heavily depend on the choice of *object representation*. For instance, if an object is represented as a point, the feature vector of the detected object is a two-dimensional coordinate vector corresponding to the center of gravity of the object in each frame.

Object detection is followed by *object tracking*. There are many approaches proposed over a number of decades (see, e.g., Yilmaz et al. (2006),) and we are interested in this proposal a statistical approach. A statistical approach assumes that the feature vector $\phi(x)$ from the object detection stage is a noisy observation of the true, underlying state (location) of the object which is not observed. The goal is to infer the underlying state for each video frame, given a sequence of observations, i.e., features vectors.

Filtering-based Visual Object Tracking In filtering-based object tracking, it is natural to establish a probabilistic graphical model, or often referred to as a state-space model, by defining

- Observation model: $p(\phi(\mathbf{x}_t)|\mathbf{z}_t)$
- Transition model: $p(\mathbf{z}_t|\mathbf{z}_{t-1})$,

where $\phi(\mathbf{x}_t)$ and \mathbf{z}_t are the observation and the latent state at time t .

One of the most well known filtering-based tracking model is so called *Kalman filter* (Broida & Chellappa, 1986). Kalman filter assume that both the observation and transition models are Gaussian distributions such that

$$\phi(\mathbf{x}_t)|\mathbf{z}_t \sim \mathcal{N}(\mathbf{W}_x\mathbf{z}_t, \mathbf{C}_x), \quad \mathbf{z}_t|\mathbf{z}_{t-1} \sim \mathcal{N}(\mathbf{W}_z\mathbf{z}_{t-1}, \mathbf{C}_z),$$

where $\mathcal{N}(\boldsymbol{\mu}, \mathbf{C})$ is a Gaussian distribution with its mean $\boldsymbol{\mu}$ and covariance matrix \mathbf{C} .

Once the model is defined, the goal is to infer the following posterior distribution:

$$p(\mathbf{z}_t|\phi(x_1), \phi(x_2), \dots, \phi(\mathbf{x}_t)). \tag{1}$$

In other words, we try to find the distribution over the potential object location in the t -th video frame given all the detected objects (represented by the feature vectors) up to the $(t - 1)$ -th frame. See Fig. 1 (a) for the graphical illustration.

In this scheme, object detection and tracking are largely considered separate from each other. This means that the object tracking stage is designed to work while being blind to the object representation or feature vectors from the object detection stage. However, this is not to say that there is no effect of the choice of object and/or feature representation, as mismatch between the model definition in object tracking and the distribution based on the selected feature representation will lead to suboptimal tracking result.

Tracking-by-Detection An approach more relevant to our proposal is *tracking-by-detection* (see, e.g., Li et al. (2013).) This approach is more holistic than the previous approach, because a single model is trained online to track an object in interest. In other words, tracking-by-detection builds a discriminative model that directly approximates the posterior distribution over the underlying location/state of the object in Eq. (1). See Fig. 1 (b) for the graphical illustration.

Often, tracking-by-detection is done not as regression but as classification of regions of a video frame. The classifier is initialized to work well on the first few frames where a separate object detector or human expert has classified each region of the frames as either foreground or background. This classifier is used to detect/track the object in the next frame of which ground-truth labeling is not available. Once each region in the next frame is classified, the classifier is further *fine-tuned* with these new examples. This continues until the video clip reaches its end or the object disappears (all regions are classified negative.)

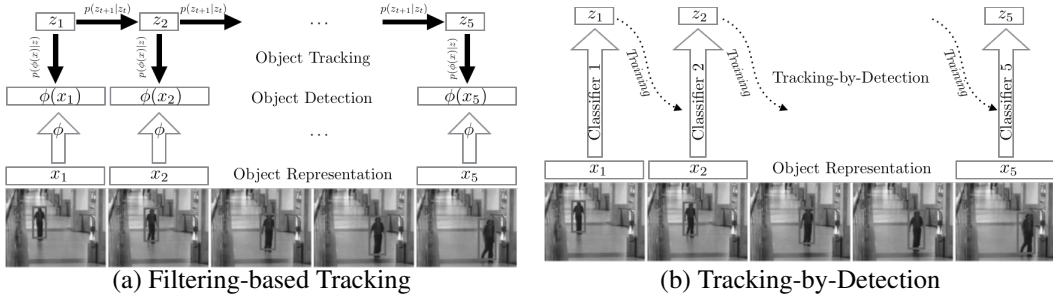


Figure 1: Graphical illustration of the filtering-based tracking and tracking-by-detection.

This approach of tracking-by-detection has a number of limitations, of which the most severe ones are drifting (accumulation of error over multiple frames) and inability to handle occlusion easily. We notice that both of these issues arise from the fact that this approach effectively assumes Markov property over the posterior distribution in Eq. (1), meaning

$$p(\mathbf{z}_t | \phi(\mathbf{x}_1), \phi(\mathbf{x}_2), \dots, \phi(\mathbf{x}_t)) \approx p(\mathbf{z}_t | \phi(\mathbf{x}_{t-1})).$$

Because the tracking model considers only two consecutive frames (or more precisely concentrates heavily on a latest pair of consecutive frames only), it is not possible for the model to adjust for accumulated error over many subsequent frames. If the model has access to the whole history of frames and its own prediction of the object’s locations, it will be possible for the model to take the errors made throughout the video clip and address the issue of drifting.

The tracking model’s lack of access to the history of the previous frames makes it nearly impossible for the model to handle occlusion. On the other hand, if the tracking model has the history of its previous observations and predictions of the object’s location, it can more easily infer that the object has not disappeared totally from the view but moved behind some other background objects. The tracking model may even be able to infer the object’s location even while it is being hidden from the view by understanding its motion based on the history the object’s locations.

Limitations We have noticed three limitations in these conventional approaches. First, *object representation is designed independently* from the rest of the tracking pipeline, and any suboptimal choice of object representation may negatively impact the subsequent stages. Second, the filtering-based approach is *not robust to a mismatch between the underlying model description and the reality*. Third, *the lack of access to the history* of all the previous video frames makes tracking-by-detection sensitive to complex motions and structured noise such as occlusion. Lastly, tracking-by-detection requires *a classifier, or a regressor, to be tuned at each frame*, making it less suitable to be applied in real-time applications.

3 VISUAL OBJECT TRACKING WITH DEEP NEURAL NETWORKS

Here we describe a novel approach to visual anonymous object tracking by using techniques from deep learning (LeCun et al., 2015). Our aim in introducing a novel approach is to build a system that avoids the four limitations of the conventional visual tracking systems we discussed in the earlier section.

The proposed model is a deep recurrent network that takes as input raw video frames of pixel intensities and returns the coordinates of a bounding box of an object being tracked for each frame. Mathematically, this is equivalent to saying that the proposed model factorizes the full tracking probability into

$$p(\mathbf{z}_1, \mathbf{z}_2, \dots, \mathbf{z}_T | \mathbf{x}_1, \mathbf{x}_2, \dots, \mathbf{x}_T) = \prod_{t=1}^T p(\mathbf{z}_t | \mathbf{z}_{<t}, \mathbf{x}_{\leq t}),$$

where \mathbf{z}_t and \mathbf{x}_t are the location of an object and an input frame, respectively, at time t . $\mathbf{z}_{<t}$ is a history of all previous locations before time t , and $\mathbf{x}_{\leq t}$ is a history of all input frames up to time t .

3.1 MODEL DESCRIPTION

At each time step t , an input frame \mathbf{x}_t is first processed by a convolutional network, which has recently become a *de facto* standard in handling visual input (see, e.g., LeCun et al., 1998; Krizhevsky et al., 2012). This results in a feature vector $\phi(\mathbf{x}_t)$ of the input frame \mathbf{x}_t :

$$\phi(\mathbf{x}_t) = \text{conv}_{\theta_c}(m(\mathbf{x}_t, \tilde{\mathbf{z}}_{t-1})), \quad (2)$$

where $\text{conv}_{\theta_c}(\cdot)$ is a convolutional network with its parameters θ_c , and $m(\cdot, \cdot)$ is a preprocessing routine for the raw frame. We will discuss this preprocessing routine at the end of this section. $\tilde{\mathbf{z}}_{t-1}$ is the predicted location of an object from the previous frame \mathbf{x}_{t-1} , which we describe in more detail below.

This feature vector of the input frame is fed into a recurrent neural network. The recurrent neural network updates its internal memory vector \mathbf{h}_t based on the previous memory vector \mathbf{h}_{t-1} , previous location of an object $\tilde{\mathbf{z}}_{t-1}$ and the current frame $\phi(\mathbf{x}_t)$:

$$\mathbf{h}_t = \text{rec}_{\theta_r}(\mathbf{h}_{t-1}, \tilde{\mathbf{z}}_{t-1}, \phi(\mathbf{x}_t)), \quad (3)$$

where rec_{θ_r} is a recurrent activation function such as gated recurrent units Cho et al. (2014), long short-term memory units Hochreiter & Schmidhuber (1997) or a simple logistic function, parametrized with the parameters θ_r . This formulation lets the recurrent neural network to summarize the history of predicted locations $\mathbf{z}_{<t}$ and input frames $\mathbf{x}_{\leq t}$ up to time step t .

With the newly updated memory state \mathbf{h}_t , the recurrent neural network computes the predictive distribution over the object’s location (see Eq. (1)). This is done again by a deep neural network out_{θ_o} Pascanu et al. (2014):

$$p(\mathbf{z}_t | \mathbf{z}_{<t}, \mathbf{x}_{\leq t}) = \text{out}_{\theta_o}(\mathbf{h}_t), \quad (4)$$

where θ_o is a set of parameters defining the output neural network. We take the mean of this predictive distribution as a predicted location $\tilde{\mathbf{z}}_t$ at time t :

$$\tilde{\mathbf{z}}_t = \mathbb{E}[\mathbf{z} | \mathbf{z}_{<t}, \mathbf{x}_{\leq t}]. \quad (5)$$

This whole process (Eqs. (2)–(5)) is iteratively applied as a stream of new frames arrives. This is graphically illustrated in Fig. 2.

Preprocessing Input Frame \mathbf{x}_t We considered a number of possible strategies for building a preprocessing routine $m(\cdot, \cdot)$ from Eq. (2). The most obvious and straightforward choice is to simply have an identity function, equivalent to simply passing a raw frame into the convolutional network conv_{θ_c} . In this case, we use an identity function to preprocess each input frame \mathbf{x}_t :

$$m(\mathbf{x}_t, \tilde{\mathbf{z}}_{t-1}) = \mathbf{x}_t, \quad (6)$$

where $\tilde{\mathbf{z}}_{t-1}$ is ignored. This is equivalent to simply letting the tracker have a full, unadjusted view of the whole frame.

On the other hand, we can design a preprocessing function m such that it will facilitate tracking. One possible choice is to weight each pixel of the raw frame \mathbf{x}_t such that a region surrounding the predicted location of an object in the previous frame is given higher weights. This will help the subsequent layers, i.e., conv_{θ_c} , rec_{θ_r} , and out_{θ_o} , to focus more on that region. We refer to this preprocessing routine as an *attentive weight scheme*.

In this model, the recurrent network outputs the coordinates of (1) top-left corner (x_0, y_0) , (2) bottom-right corner (x_1, y_1) , (3) log-scale s , (4) log-ratio r between the stride and the image size, and (5) log-amplitude a . Given these output, we weight each pixel using a mixture of $N \times N$ Gaussians. Each Gaussian (i, j) is centered at

$$\left(\frac{x_0 + x_1}{2} + \left(i - \frac{N}{2} - 0.5 \right) \exp(r)K, \frac{y_0 + y_1}{2} + \left(j - \frac{N}{2} - 0.5 \right) \exp(r)K \right),$$

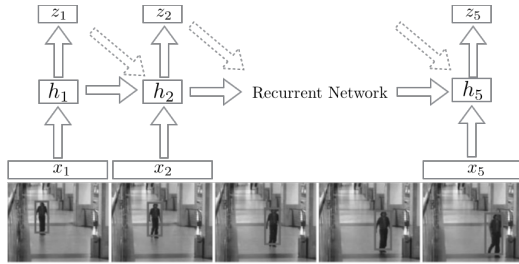


Figure 2: Graphical illustration of the visual tracking system proposed here.

and has the standard deviation of $\exp(s) \frac{K}{2}$. K corresponds to the width or height of a frame. These Gaussians are used to form a mask $G(\mathbf{z}_{t-1})$ which is used as

$$m(\mathbf{x}_t, \mathbf{z}_{t-1}) = \mathbf{x}_t \cdot G(\mathbf{z}_{t-1}) \quad (7)$$

We emphasize that we only weight the pixels of each frame and do *not* extract a patch, as was done by Gregor et al. (2015) and Kahou et al. (2015), because this approach of ignoring an out-of-patch region may lose too much information needed for tracking.

3.2 TRAINING

Unlike the existing approaches to visual object tracking, described in Sec. 2, we take an off-line training strategy. This means that the trained model is used as is in test time.

An obvious advantage to this approach is that there is no overhead in finetuning the model on-the-fly during test time. On the other hand, there is an obvious disadvantage that the model must be able to track an object whose shape or texture information was *not* available during training time. We propose here a training strategy that aims at overcoming this disadvantage.

We were motivated from recent observations from many research groups that a deep convolutional network, pretrained on a large image dataset of generic, natural images, is useful for subsequent vision tasks which may not necessarily involve the same types of objects (see, e.g., Sermanet et al., 2013; Bar et al., 2015). As the model we propose here consists of a convolutional network and recurrent network, we expect a similar benefit by training the whole model with generic shapes, which may not appear during test time.

As usual when training a deep neural network, we use stochastic gradient descent (SGD). At each SGD update, we *generate* a minibatch of examples by the following steps:

1. Select a random background image from a large set of image.
2. Randomly choose a shape of an object from a predefined set of generic shapes.
3. Create a sequence of frames by randomly moving the selected object with cluttered background and foreground.
4. (Optional) Add various types of noise, including motion and scale change of both object and clutters.

After these steps, each training example is a pair of a video clip, which contains a randomly chosen background and a moving shape, and a sequence of ground-truth locations, i.e., $((\mathbf{x}_1, \mathbf{z}_1^*), \dots, (\mathbf{x}_T, \mathbf{z}_T^*))$.

We use this minibatch of N generated examples to compute the gradient of the minibatch log-likelihood \mathcal{L} , where

$$\mathcal{L}(\theta_c, \theta_r, \theta_o) = \frac{1}{N} \sum_{n=1}^N \sum_{t=k+1}^T \log p(\mathbf{z}_t^n = \mathbf{z}_t^{*,n} | \mathbf{z}_{<t}^{*,n}, \mathbf{x}_{\leq t}^n).$$

As this is an anonymous object tracking system, the model is given the ground-truth locations of the object for the first k frames.

Another training criterion is possible, if our prediction $\tilde{\mathbf{z}}_t$ as each step t is a differentiable function. In this case, we let the model freely track an object given a training video sequence and maximize the log-probability of the ground-truth location *only* at the last frame:

$$\mathcal{L}(\theta_c, \theta_r, \theta_o) = \frac{1}{N} \sum_{n=1}^N \log p(\mathbf{z}_T^n = \mathbf{z}_T^{*,n} | \tilde{\mathbf{z}}_{<T}^n, \mathbf{x}_{\leq T}^n). \quad (8)$$

According to our preliminary experiments, we use this second strategy throughout this paper.

Of course, in this case, there is no guarantee that any intermediate prediction made by the model correspond to the correct object location. To avoid this issue, we add the following auxiliary cost to

We can use, for instance, ImageNet Data from <http://www.image-net.org/>, or create one with random clutters as in MNIST cluttered from <https://github.com/deepmind/mnist-cluttered>.

the new cost above:

$$\tilde{\mathcal{L}}(\theta_c, \theta_r, \theta_o) = \frac{1}{N} \sum_{n=1}^N \sum_{t=k+1}^T \log p(\mathbf{z}_t^n = \mathbf{z}_t^{*,n} | \tilde{\mathbf{z}}_{<t}^n, \mathbf{x}_{\leq t}^n). \quad (9)$$

Minimizing this auxiliary cost encourages the model to following the object in the intermediate frames.

In our case, the model predicts two points $\mathbf{z}_t = [x_0, y_0, x_1, y_1]$ in the input frame which corresponds to the top-left (x_0, y_0) and bottom-right (x_1, y_1) corners of a bounding box. We use a Gaussian distribution with an fixed, identity covariance matrix, whose mean is computed from \mathbf{h}_t (see Eq. (3).) In order to reduce variance, we do not sample from this distribution, but simply take the mean as the prediction:

$$\tilde{\mathbf{z}}_t = \mathbb{E}[\mathbf{z}_t | \tilde{\mathbf{z}}_{<T}, \mathbf{x}_{\leq T}].$$

This effectively reduces the auxiliary cost in Eq. (9) as well as the main cost in Eq. (8) to a mean-squared error.

In the case of using the modified selective attention model to preprocess the input frame, there are two additional output elements which are the standard deviation σ and the stride δ . As we consider both of these as real values, this simply makes the predictive distribution to be a six-dimensional vector, i.e., $\dim(\mathbf{z}_t) = 4$.

3.3 CHARACTERISTICS

There are three main characteristics that set the proposed approach apart from the previous works on visual object tracking.

First, the proposed model is trained end-to-end, including object representation extraction, object detection and object tracking. The model works directly on the raw pixel intensities of each frame. This is unlike conventional object tracking systems, in which appearance modeling is considered largely separate from the actual tracking system (see, e.g., Li et al., 2013). This largely prevents potential performance degradation from having suboptimal, hand-engineered object representation and detector.

Second, the proposed model works with anonymous objects by design. As we train a model with a large set of generic-shaped objects offline, the model learns to detect a generic object that was pointed out initially rather than to detect a certain, predefined set of objects. As the proposed model is a recurrent neural network which can maintain the history of the object’s trajectory, it implicitly learns to find a region in an input frame which has a similar activation pattern from the previous frames. In fact, human babies are known to be able to track objects even before having an ability to classify it into one of the object categories (Ruff & Rothbart, 2001).

Lastly, training is done fully off-line. We note first that this is both an advantage and disadvantage of the proposed approach. This off-line training strategy is advantageous in test time, as there is no need to re-tune any part of the system. As the model parameters are fixed during test time, it will be more straightforward to implement the trained model on a hardware, achieving a desirable level of power consumption and speed (Farabet et al., 2011). On the other hand, this implies that the proposed system lacks the adaptability to novel objects that are novel w.r.t. the shapes used during training, which is exactly a property fully exploited by any existing tracking-by-detection visual tracking system.

3.4 RELATED WORK

As we were preparing this work, Kahou et al. (2015) independently proposed a similar visual object tracker based on a recurrent neural network. Here let us describe the similarities and differences between their recurrent attentive tracking model (RATM) with the proposed tracking approach.

A major common feature between these two approaches is that both of these use a recurrent neural network as a main component. A major difference between the RATM and the proposed approach is in training. Both the RATM and the model proposed in this paper use the intermediate locations of an object as an auxiliary target (see Eq. (9).) Kahou et al. (2015) report that this use of auxiliary

cost stabilized the tracking quality, which is further confirmed by our experiments presented later in this paper.

A major difference is that Kahou et al. (2015) used a classification error, averaged over all the frames, as a final cost, while we propose to use the final localization error. Furthermore, they use the selective attention mechanism from (Gregor et al., 2015), allowing the RATM only a small sub-region of the whole canvas at each frame. This is contrary to the recurrent visual tracker proposed in this paper which has access to the full frame every time.

Earlier, Denil et al. (2012) proposed a visual object tracking system based on deep neural networks. Their model can be considered as an intermediate step away from the conventional tracking approaches toward the one proposed here and by Kahou et al. (2015). They used a restricted Boltzmann machine (Smolensky, 1986) as an object detection model together in a filtering-based visual tracking (state-space model with particle filtering for inference.)

Although they are not specifically for visual object tracking, two recent works on image/video description generation tasks have shown that a recurrent network, together with a convolutional network, is able to attend (detect and localize) to objects in both an image and a video clip (Xu et al., 2015; Yao et al., 2015). Similarly, Mnih et al. (2014) and Ba et al. (2014) showed that a recurrent network tracks an object if it were trained to classify an object, or multiple objects, in an image.

4 DATA GENERATION

We evaluate the proposed approach of visual anonymous object tracking on artificially generated datasets. We vary the configurations of generating these datasets to make sure that the following empirical evaluations support our claim and conjectures about the proposed model.

All the datasets are based on the cluttered MNIST. Each video sequence used for training consists of 20 frames, and each frame is 100×100 large. The cluttered MNIST was chosen as a basis of generating further datasets, as one of the most important criterion we aim to check with the proposed approach is the robustness to noise. In order to make sure that these clutters acts as both background noise and as objects hindering the sight of the models, we put some clutters in a background layer and the others in a foreground layer (overshadowing the target object.) Furthermore, the clutters move rather than stay in the initial positions to make it more realistic.

The target has a random initial velocity (v_{x_0}, v_{y_0}) and position (x_0, y_0) . At each time frame, the position is changed by $(\Delta x_t, \Delta y_t) = (kv_{x,t-1}, kv_{y,t-1})$ where k is a hyper-parameter (0.1 in our experiments) correlated to the frame rate. We change the velocity by $(\Delta v_{x,t}, \Delta v_{y,t}) \sim \mathcal{N}(0, v'I)$, where $v' = 0.1$ is a hyper-parameter controlling the scale of velocity changes. This change in the velocity introduces acceleration, making it more difficult for a tracking system.

To ensure that our dataset is as realistic as possible, we include other transformations. For example, at each time step, the target changes its scale by a random factor $f = p \exp(\tilde{f})$, where $\tilde{f} \sim \mathcal{U}(-0.5, 0.5)$ and $p = 0.1$ controls the magnitude of scale change. Finally, the intensities of each clutter and the moving MNIST digit are uniform-randomly scaled between 64 and 255 (before normalization.)

Multiple Digits We evaluate our model on two different cases. In the first case, there is only a single digit moving around in each video sequence. Although there are clutters in the background/foreground, this setting is sufficiently easy and can be considered as a sanity check. We call this dataset **MNIST-Single-Same**.

The second dataset, **MNIST-Multi-Same**, contains frames of which each contains more than one digits. More specifically, we generate each video sequence such that there are two digits simultaneously moving around. In order for the tracking system to work well, the system needs to be able to detect the characteristics of the object in interest from the first few frames (when the ground-truth locations are given) and maintain it throughout the sequence.

Novel Test Digit Classes As our goal is to build an *anonymous* object tracking system. We evaluate a trained model with sequences containing objects that do not appear during training time.

<https://github.com/deepmind/mnist-cluttered>

More specifically, we test the models on two sets of sequences containing one or two MNIST-2 digits, where one MNIST-2 digit is created by randomly overlapping two randomly selected normal MNIST digits on top of each other (Wang et al., 2014). We call these datasets **MNIST-Single-Diff** and **MNIST-Multi-Diff**, respectively.

Generalization to Longer Video Sequence In all the cases, we evaluate a trained model on test sequences that are longer than the training sequences. This is a necessary check for any model based on recurrent neural networks, as some recent findings suggest that on certain tasks recurrent neural networks fail to generalize to longer test sequences (Joulin & Mikolov, 2015; Grefenstette et al., 2015). We vary the lengths of test sequences among $\{20, 40, 80, 160\}$, while all the models are trained with 20-frame-long training sequences.

5 MODELS AND TRAINING

We test five models on each of the four cases, **MNIST- $\{\text{Single, Multi}\}$ - $\{\text{Same, Diff}\}$** .

Recurrent Visual Object Tracker (RecTracker-X) The first model, **RecTracker-ID**, is the proposed recurrent visual object tracker (see Sec. 3.1.) The tracker has a full, unadjusted view of the whole frame. Alternatively, the tracker with attentive weight scheme imposes weighting mask of $N \times N$ Gaussian filters. In this paper, We evaluate **RecTracker-Att-1** and **RecTracker-Att-3**, where N is 1 and 3 respectively.

Convolutional Network Only Tracker (ConvTracker) The third model is a simpler variant of the proposed model where the recurrent network is omitted from the proposed recurrent visual tracking model. Instead, this model considers four frames (three preceding frames + current frame) and predict the location of an object at the current frame. We only test the identity preprocessing routine in Eq. (6). We call this model **ConvTracker**. Other than the omission of the recurrent network, all the other details are identical to those of RecTracker-ID, RecTracker-Att-1 and RecTracker-Att-3.

Kernelized Correlation Filters based Tracker (KerCorrTracker) Lastly, we use the kernelized correlation filters-based visual tracker proposed by Henriques et al. (2015). This is one of the state-of-the-art visual object tracking systems and follows a tracking-by-detection strategy (see Sec. 2.) This third model is chosen to highlight the differences between the existing tracking approaches and the proposed one.

5.1 NETWORK ARCHITECTURES

We describe the architectures of each network–convolutional and recurrent networks– in Appendix A.

5.2 TRAINING

We describe the architectures of each network–convolutional and recurrent networks– in Appendix B.

6 RESULT AND ANALYSIS

6.1 EVALUATION METRIC

We use the intersection-over-union (IOU) as an evaluation metric. The IOU is defined as

$$\text{IOU}(\mathbf{z}_t^*, \tilde{\mathbf{z}}_t) = \frac{|M^* \cap \tilde{M}|}{|M^* \cup \tilde{M}|},$$

where M^* and \tilde{M} are binary masks whose pixels inside a bounding box (either ground-truth * or predicted $\tilde{}$) are 1 and otherwise 0. A higher IOU implies better tracking quality, and it is bounded between 0 and 1. For each video sequence, we compute the average IOU across all the frames.

<http://home.isr.uc.pt/~henriques/circulant/>

6.2 QUANTITATIVE ANALYSIS

Test Seq. Length	ConvTracker				RecTracker-ID			
	20	40	80	160	20	40	80	160
MNIST-Single-Same	0.36 ± 0.12	0.35 ± 0.11	0.33 ± 0.10	0.29 ± 0.10	0.61 ± 0.11	0.61 ± 0.11	0.58 ± 0.12	0.53 ± 0.13
MNIST-Single-Diff	0.37 ± 0.13	0.35 ± 0.11	0.33 ± 0.10	0.29 ± 0.10	0.48 ± 0.08	0.49 ± 0.09	0.48 ± 0.08	0.46 ± 0.10
MNIST-Multi-Same	0.17 ± 0.11	0.15 ± 0.09	0.14 ± 0.08	0.13 ± 0.08	0.36 ± 0.20	0.31 ± 0.19	0.28 ± 0.18	0.26 ± 0.17
MNIST-Multi-Diff	0.17 ± 0.13	0.15 ± 0.11	0.14 ± 0.10	0.13 ± 0.10	0.33 ± 0.14	0.29 ± 0.14	0.26 ± 0.13	0.24 ± 0.12

Table 1: Average and standard deviation of IOU’s computed over 500 test sequences using the ConvTracker and RecTracker-ID with different datasets and different lengths of test sequences. From this table, it is clear that the RecTracker-ID performs better than the ConvTracker which does not have a recurrent network unlike the RecTracker-ID.

Importance of Recurrent Network First, we compare the **ConvTracker** and **RecTracker-ID**. They both use the identity preprocessing routine, and the only difference is that the latter has a recurrent network while the former does not. The results, in terms of the average IOU, are presented in Table 1.

In this table, the importance of having a recurrent layer is clearly demonstrated. Across all the cases—different data configurations and test sequence lengths—the RecTracker-ID significantly outperforms the ConvTracker. Also, we notice that the tracking quality degrades as the length of test sequences increases (up to 8 folds.)

Test Seq. Length	RecTracker-ID				RecTracker-Att-1			
	20	40	80	160	20	40	80	160
MNIST-Single-Same	0.61 ± 0.11	0.61 ± 0.11	0.58 ± 0.12	0.53 ± 0.13	0.59 ± 0.14	0.58 ± 0.14	0.54 ± 0.14	0.48 ± 0.15
MNIST-Single-Diff	0.48 ± 0.08	0.49 ± 0.09	0.48 ± 0.08	0.46 ± 0.10	0.64 ± 0.06	0.64 ± 0.06	0.61 ± 0.07	0.56 ± 0.09
MNIST-Multi-Same	0.36 ± 0.20	0.31 ± 0.19	0.28 ± 0.18	0.26 ± 0.17	0.37 ± 0.22	0.35 ± 0.22	0.29 ± 0.22	0.25 ± 0.20
MNIST-Multi-Diff	0.33 ± 0.14	0.29 ± 0.14	0.26 ± 0.13	0.24 ± 0.12	0.41 ± 0.19	0.35 ± 0.18	0.31 ± 0.17	0.28 ± 0.16

Table 2: Average and standard deviation of IOU’s computed over 500 test sequences using the RecTracker-ID and RecTracker-Att-1. The results by **RecTracker-ID** are identical to those in Table 1.

Effect of Attentive Weight Scheme Next, we evaluate the effect of the attentive weight scheme (see Eq. (7) and surrounding text) against the simple identity preprocessing scheme (see Eq. (6) and surrounding text.) From Table 2, we notice an interesting pattern. When the training and test shapes are of the same classes (similar shapes), it is better to use the identity preprocessing scheme (**RecTracker-ID**). On the other hand, **RecTracker-Att-1** outperforms the simpler one, when the shapes are different between training and test.

Test Seq. Length	RecTracker-Att-1				RecTracker-Att-3			
	20	40	80	160	20	40	80	160
MNIST-Single-Same	0.59 ± 0.14	0.58 ± 0.14	0.54 ± 0.14	0.48 ± 0.15	0.57 ± 0.14	0.55 ± 0.14	0.53 ± 0.15	0.47 ± 0.15
MNIST-Multi-Same	0.37 ± 0.22	0.35 ± 0.22	0.29 ± 0.22	0.25 ± 0.20	0.36 ± 0.22	0.32 ± 0.21	0.27 ± 0.21	0.24 ± 0.19
MNIST-Single-Diff	0.64 ± 0.06	0.64 ± 0.06	0.61 ± 0.07	0.56 ± 0.09	0.61 ± 0.06	0.61 ± 0.06	0.59 ± 0.06	0.56 ± 0.10
MNIST-Multi-Diff	0.41 ± 0.19	0.35 ± 0.18	0.31 ± 0.17	0.28 ± 0.16	0.38 ± 0.17	0.33 ± 0.17	0.30 ± 0.16	0.27 ± 0.16

Table 3: Average and standard deviation of IOU’s computed over 500 test sequences using the RecTracker-Att-1 and RecTracker-Att-3

Comparison between different N We then compare **RecTracker-Att-1** with **RecTracker-Att-3**. As shown in Table 3, the performance between the two models did not differ that much. As it turns out, as long as the center Gaussian filter focuses on the target, the model has not motivation to adjust the other ones. Manual inspection reveal these “outer” filters are often placed outside the canvas. In Fig. 3, we show the attention weights computed by **RecTracker-Att-1** and **RecTracker-Att-1**. Evidently, only one Gaussian is being used.

Comparison against Tracking-by-Detection Table 4 compares the tracking quality between the proposed recurrent tracking model **RecTracker-Att-1** and the kernelized correlation filters based one **KerCorrTracker** by Henriques et al. (2015). We observe that **RecTracker-Att-1** outperforms the **KerCorrTracker** when there’s only a single object in a test sequence. However, when there are

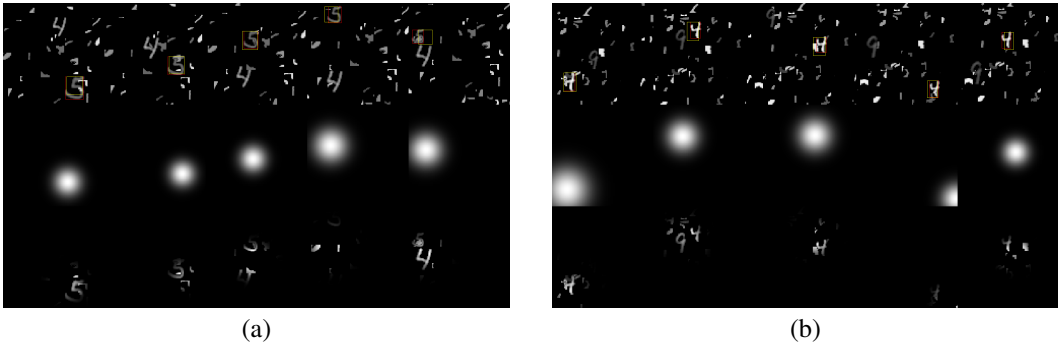


Figure 3: (a) RecTracker-Att-1 and (b) RecTracker-Att-3. Image sequence, label and prediction shown at the top row, while the masks are shown at middle, and the masked images are shown at bottom. The mask patterns look alike between models.

Test Seq. Length	RecTracker-Att-1				KerCorrTracker			
	20	40	80	160	20	40	80	160
MNIST-Single-Same	0.59 ± 0.14	0.58 ± 0.14	0.54 ± 0.14	0.48 ± 0.15	0.37 ± 0.28	0.29 ± 0.26	0.20 ± 0.22	0.13 ± 0.15
MNIST-Multi-Same	0.37 ± 0.22	0.35 ± 0.22	0.29 ± 0.22	0.25 ± 0.20	0.41 ± 0.26	0.32 ± 0.26	0.24 ± 0.23	0.16 ± 0.17
MNIST-Single-Diff	0.64 ± 0.06	0.64 ± 0.06	0.61 ± 0.07	0.56 ± 0.09	0.54 ± 0.27	0.47 ± 0.28	0.36 ± 0.26	0.25 ± 0.22
MNIST-Multi-Diff	0.41 ± 0.19	0.35 ± 0.18	0.31 ± 0.17	0.28 ± 0.16	0.55 ± 0.27	0.46 ± 0.27	0.34 ± 0.24	0.23 ± 0.20

Table 4: Average and standard deviation of IOU’s computed over 500 test sequences using the RecTracker-Att-1 and KerCorrTracker with MNIST-1 and MNIST-2 test sets and different lengths of test sequences.

two objects in a sequence and the model was asked to track only one of them, the **RecTracker-Att-1** and **KerCorrTracker** perform comparably, but only do so with shorter sequences. Tracking-by-detection focuses exclusively on local region and get less distracted. However, longer sequences have higher probability of distraction (by either clutter or another digit). Consequently, retaining longer history allows our model to steer towards our target better. Finally, one noticeable difference is that standard deviation of **RecTracker-Att-1** is one order of magnitude smaller, indicating a much tighter tracking.

Putting these results together, we note the followings. The under-performing **ConvTracker** clearly demonstrates that it is important for a tracking model to be capable of capturing temporal dynamics. Among the proposed recurrent tracking models, the **RecTracker-ID** performs better when the same types of objects are used both during training and test, but in the other case the **RecTracker-Att-1** does better. This is similar to the observation we made when these models were tracking a single object.

We however remind readers that these results should be taken with a grain of salt. It is unclear how the proposed tracking model can be extended to track arbitrarily many objects. Also, a more accurate comparison between the proposed models and tracking-by-detection needs to involve natural scenes, real objects and dynamics. Under such scenarios, many extensions are called for in order to make the model robust. We leave this as future research.

6.3 VISUALIZATION OF TRACKING

We have prepared video clips of tracking results by all the tested models at <http://barclayii.github.io/tracking-with-rnn>. See Fig. 4 for one such example.

Our visual inspection reveals that

1. In most cases **ConvTracker** fail at tracking an anonymous object. This suggests the importance of having an explicit memory which is lacking from the **ConvTracker**.
2. Although the quantitative analysis based on IOU, **RecTracker-ID** almost always underperforms compared to **RecTracker-Att-N**’s, the qualitative analysis reveals that it still tracks an object fairly well. This suggests that the IOU may not be the optimal measure of tracking quality.

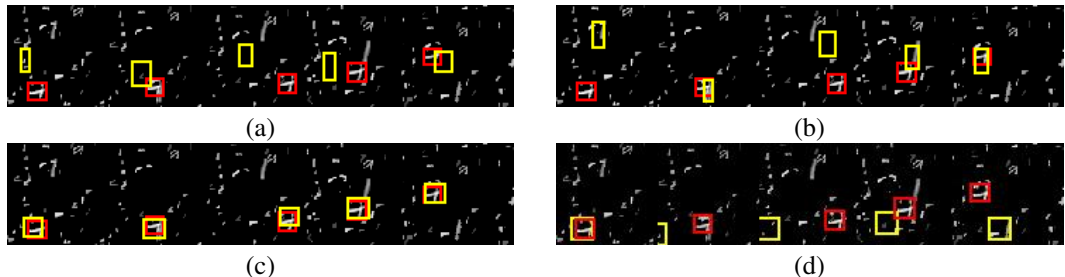


Figure 4: (a) ConvTracker, (b) RecTracker-ID, (c) RecTracker-Att-1 and (d) KerCorrTracker

3. **RecTracker-Att- N** 's often confuse the object being tracked, and this happens especially when another brighter object passes nearby. This may be due to the fact that the masking with Gaussian attentive is too simplistic: it penalizes darker pixels more than brighter ones, making a brighter object stand out more.

7 CONCLUSION

In this paper, we proposed an end-to-end trainable visual object tracking model based on convolutional and recurrent neural networks. Unlike conventional tracking approaches, the full pipeline of visual tracking—object representation, object extraction and location prediction— is jointly tuned to maximize the tracking quality. The proposed tracking model combines many recent advances in deep learning and was found to well perform on challenging, artificially generated sequences.

We consider this work as a first step toward building a full end-to-end trainable visual object tracking system. There are a number of issues to be investigated and resolved in the future. First, the proposed models must be evaluated on natural scenes with real objects and their dynamics. Second, there needs to be research on algorithms to adapt a pre-trained model online. Third, we need to find a network architecture that can track an arbitrary number of objects without a predefined upper limit.

REFERENCES

- Ba, Jimmy, Mnih, Volodymyr, and Kavukcuoglu, Koray. Multiple object recognition with visual attention. *arXiv preprint arXiv:1412.7755*, 2014.
- Bar, Yaniv, Diamant, Idit, Wolf, Lior, and Greenspan, Hayit. Deep learning with non-medical training used for chest pathology identification. In *SPIE Medical Imaging*, pp. 94140V–94140V. International Society for Optics and Photonics, 2015.
- Broida, Ted J and Chellappa, Rama. Estimation of object motion parameters from noisy images. *Pattern Analysis and Machine Intelligence, IEEE Transactions on*, (1):90–99, 1986.
- Cho, Kyunghyun, Van Merriënboer, Bart, Gulcehre, Caglar, Bahdanau, Dzmitry, Bougares, Fethi, Schwenk, Holger, and Bengio, Yoshua. Learning phrase representations using rnn encoder-decoder for statistical machine translation. *arXiv preprint arXiv:1406.1078*, 2014.
- Denil, Misha, Bazzani, Loris, Larochelle, Hugo, and de Freitas, Nando. Learning where to attend with deep architectures for image tracking. *Neural computation*, 24(8):2151–2184, 2012.
- Farabet, Clément, LeCun, Yann, Kavukcuoglu, Koray, Culurciello, Eugenio, Martini, Berin, Aksele, Polina, and Talay, Selcuk. Large-scale fpga-based convolutional networks. *Machine Learning on Very Large Data Sets*, 1, 2011.
- Graves, Alex. Generating sequences with recurrent neural networks. *arXiv preprint arXiv:1308.0850*, 2013.
- Grefenstette, Edward, Hermann, Karl Moritz, Suleyman, Mustafa, and Blunsom, Phil. Learning to transduce with unbounded memory. *arXiv preprint arXiv:1506.02516*, 2015.

- Gregor, Karol, Danihelka, Ivo, Graves, Alex, and Wierstra, Daan. Draw: A recurrent neural network for image generation. *arXiv preprint arXiv:1502.04623*, 2015.
- Henriques, J. F., Caseiro, R., Martins, P., and Batista, J. High-speed tracking with kernelized correlation filters. *Pattern Analysis and Machine Intelligence, IEEE Transactions on*, 2015. doi: 10.1109/TPAMI.2014.2345390.
- Hochreiter, Sepp and Schmidhuber, Jürgen. Long short-term memory. *Neural computation*, 9(8): 1735–1780, 1997.
- Joulin, Armand and Mikolov, Tomas. Inferring algorithmic patterns with stack-augmented recurrent nets. *arXiv preprint arXiv:1503.01007*, 2015.
- Kahou, Samira Ebrahimi, Michalski, Vincent, and Memisevic, Roland. Ratm: Recurrent attentive tracking model. *arXiv preprint arXiv:1510.08660*, 2015.
- Krizhevsky, Alex, Sutskever, Ilya, and Hinton, Geoffrey E. Imagenet classification with deep convolutional neural networks. In *Advances in neural information processing systems*, pp. 1097–1105, 2012.
- LeCun, Yann, Bengio, Yoshua, and Hinton, Geoffrey. Deep learning. *Nature*, 521(7553):436–444, 2015.
- LeCun, Yann A, Bottou, Léon, Orr, Genevieve B, and Müller, Klaus-Robert. Efficient backprop. In *Neural networks: Tricks of the trade*, pp. 9–48. Springer, 1998.
- Li, Xi, Hu, Weiming, Shen, Chunhua, Zhang, Zhongfei, Dick, Anthony, and Hengel, Anton Van Den. A survey of appearance models in visual object tracking. *ACM transactions on Intelligent Systems and Technology (TIST)*, 4(4):58, 2013.
- Mnih, Volodymyr, Heess, Nicolas, Graves, Alex, and Kavukcuoglu, Koray. Recurrent models of visual attention. In Ghahramani, Z., Welling, M., Cortes, C., Lawrence, N.D., and Weinberger, K.Q. (eds.), *Advances in Neural Information Processing Systems 27*, pp. 2204–2212. Curran Associates, Inc., 2014. URL <http://papers.nips.cc/paper/5542-recurrent-models-of-visual-attention.pdf>.
- Pascanu, Razvan, Gulcehre, Caglar, Cho, Kyunghyun, and Bengio, Yoshua. How to construct deep recurrent neural networks. In *International Conference on Learning Representation (ICLR)*, 2014.
- Ruff, Holly Alliger and Rothbart, Mary Klevjord. *Attention in early development: Themes and variations*. Oxford University Press, 2001.
- Sermanet, Pierre, Eigen, David, Zhang, Xiang, Mathieu, Michaël, Fergus, Rob, and LeCun, Yann. Overfeat: Integrated recognition, localization and detection using convolutional networks. *arXiv preprint arXiv:1312.6229*, 2013.
- Smolensky, P. Information processing in dynamical systems: foundations of harmony theory. In *Parallel distributed processing: explorations in the microstructure of cognition, vol. 1: foundations*, pp. 194–281. MIT Press, Cambridge, MA, USA, 1986.
- Wang, Qian, Zhang, Jiaying, Song, Sen, and Zhang, Zheng. Attentional neural network: Feature selection using cognitive feedback. In Ghahramani, Z., Welling, M., Cortes, C., Lawrence, N.D., and Weinberger, K.Q. (eds.), *Advances in Neural Information Processing Systems 27*, pp. 2033–2041. Curran Associates, Inc., 2014.
- Xu, Kelvin, Ba, Jimmy, Kiros, Ryan, Cho, Kyunghyun, Courville, Aaron, Salakhutdinov, Ruslan, Zemel, Richard, and Bengio, Yoshua. Show, attend and tell: Neural image caption generation with visual attention. In *International Conference on Machine Learning*, 2015.
- Yao, Li, Torabi, Atousa, Cho, Kyunghyun, Ballas, Nicolas, Pal, Christopher, Larochelle, Hugo, and Courville, Aaron. Describing videos by exploiting temporal structure. In *International Conference on Computer Vision*, 2015.
- Yilmaz, Alper, Javed, Omar, and Shah, Mubarak. Object tracking: A survey. *Acm computing surveys (CSUR)*, 38(4):13, 2006.

A NETWORK ARCHITECTURES

Convolutional Network We use a single convolutional layer with 32 10×10 filters. These filters are applied with stride 5 to the input frame. As it is important to maintain as much spatial information as possible for tracking to work well, we do not use any pooling. This convolutional layer is immediately followed by an element-wise tanh.

In the case of **ConvTracker**, a fully-connected layer with 200 tanh units follows the convolutional layer. This fully-connected layer also receives as the input the predicted locations of the four preceding frames.

Recurrent Network We use 200 gated recurrent units (GRU, Cho et al., 2014) to build a recurrent network. At each time step, the activation of the convolutional layer (see above) and the predicted object location $\tilde{\mathbf{z}}_{t-1}$ in the previous frame are fed into the recurrent network.

B TRAINING

We train each model up to 50 epochs, or until the training cost stops improving, using a training set of 3,200,000 randomly-generated examples. We use RMSProp, which was implemented according to (Graves, 2013), with minibatches of size 32 examples.